High-Altitude Cosmic-Ray Neutron Intensity Variations*

ROBERT K. SOBERMAN†‡
New York University, New York, New York

(Received October 24, 1955; revised manuscript received February 2, 1956)

Three groups of balloon flights carrying unshielded boron trifluoride counters were made from geomagnetic latitudes 10.1°N, 55.1°N, and 88.6°N. From the data obtained, curves of slow-neutron intensity *versus* atmospheric depth for depths less than 700 millibars are plotted. The mean absorption lengths for neutrons in the equilibrium portion of the atmosphere were found to be $L(10.1°)=212$ g/cm², $L(55.1°)=164$ g/cm², and $L(88.6°)=164$ g/cm². The depths of the neutron intensity maxima were found to be $\theta_{max}(10.1°)=120\pm5$ mb, $\theta_{max}(55.1°)=100\pm5$ mb, $\theta_{max}(88.6°)=75\pm5$ mb. From these results and those of other investigators, the variation of the mean absorption coefficient ($\mu=1/L$) and the depth of the neutron intensity maximum are plotted as functions of the geomagnetic latitude. A family of curves of neutron intensity *versus* atmospheric depth is drawn for geomagnetic latitudes at 10-degree intervals between 0° and 90°N, and from this the low-energy neutron capture per square centimeter per second by the $N^{14}(n,p)$ reaction in the atmosphere is calculated and plotted as a function of geomagnetic latitude. It is found that the observed neutron intensity varies by about 420% from 0° to 90°N. A value of 5.8×10^{18} sec^{-1} is obtained for the total number of low-energy neutrons captured in the atmosphere.

INTRODUCTION

COSMIC-RAY neutron intensities have been measured as a function of atmospheric pressure at three different latitudes. These measurements were made in the range of 20 to 700 millibars[1] using boron trifluoride counters flown by means of large polyethelene balloons. The experiments covered the period from August, 1952 to September, 1954. A preliminary account of one of the measurements has already been given.[2] This is a continuation of the work at this laboratory of several investigators[3–5] to determine the latitude effect on cosmic-ray neutrons.

From the studies of cosmic-ray neutrons,[6] one may summarize those results which have been reasonably well established as follows:

(1) The bulk of the observed cosmic-ray neutrons are secondary particles produced as a result of charged primaries colliding with nuclei in our atmosphere. Measurements of the half-life of the neutron[7,8] would indicate that no primary neutrons could come from outside the solar system because they would decay before reaching the earth. The lack of any large diurnal effect in the neutron intensity[9] indicates that there are few, if any, primary neutrons reaching the earth from the sun.

(2) These neutrons are produced with all energies up to the primary particle energies when energetic primaries and secondaries interact with the oxygen and nitrogen nuclei. They are then slowed down and captured by further interaction with the oxygen and nitrogen nuclei in the atmosphere.[10]

(3) There appears to be a close correspondence between the altitude and latitude intensity variations of fast (2–30 Mev) and slow (<1 ev) neutrons.[11]

(4) There is a large geomagnetic latitude dependence in the neutron intensity distribution at any one atmospheric pressure.[11,12]

(5) At atmospheric pressures ranging from 200 to 600 or 700 millibars, the neutron intensity varies approximately exponentially[3–5,10,11,13] according to the formula $N=N_0e^{-p/L}$, where p is the atmospheric pressure or depth, and L is the mean absorption length in the units of p. In this region of the atmosphere there is an equilibrium established between neutron production and absorption.[10]

(6) The value of the mean absorption length (L) varies with the geomagnetic latitude.[11]

(7) There is a maximum in the neutron intensity when plotted as a function of atmospheric pressure.[13] There is a shift in the position of this maximum with changing geomagnetic latitude.[14]

The objective of the present experiments was to determine the variation of the slow-neutron absorption rate in the atmosphere with altitude and latitude, using the data of some of the investigators referred to above in addition to the data presented here. From these variations, a world-wide picture of cosmic-ray neutron intensity could be constructed, and from this the total number of cosmic-ray neutrons produced in the atmosphere could be evaluated.

* Supported by a joint program of the Office of Naval Research and the U. S. Atomic Energy Commission.

† This report is an abridgment of a dissertation submitted in partial fulfillment of the requirements for the degree of Doctor of Philosophy at New York University, 1955.

‡ Now with the General Electric Company, Schenectady, New York.

[1] 1 mb = 1.02 g/cm².
[2] Neuburg, Soberman, Swetnick, and Korff, Phys. Rev. **97**, 1276 (1955).
[3] W. P. Staker, Phys. Rev. **80**, 52 (1950).
[4] W. O. Davis, Phys. Rev. **80**, 150 (1950).
[5] Staker, Pavalow, and Korff, Phys. Rev. **81**, 889 (1951).
[6] For example, see references contained in reference 3.
[7] J. M. Robson, Phys. Rev. **77**, 747 (1950).
[8] A. H. Snell and L. C. Miller, Phys. Rev. **74**, 1217 (1948).
[9] Fonger, Firor, and Simpson, Phys. Rev. **89**, 891 (1953).
[10] Bethe, Korff, and Placzek, Phys. Rev. **57**, 573 (1940).
[11] J. A. Simpson, Phys. Rev. **83**, 1175 (1951).
[12] L. C. L. Yuan, Phys. Rev. **76**, 1267 (1949).
[13] L. C. L. Yuan, Phys. Rev. **81**, 175 (1951).
[14] Soberman, Beiser, and Korff, Phys. Rev. **100**, 859 (1955).

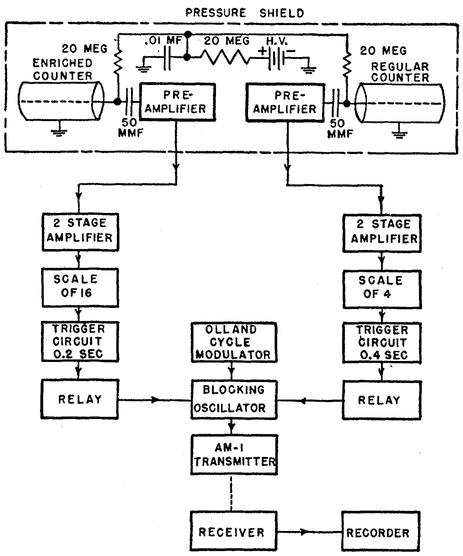

FIG. 1. Block diagram of the flight frame and receiving apparatus.

APPARATUS

To measure the neutron intensity as a function of atmospheric pressure, boron trifluoride counters with suitable electronic circuitry were flown by means of large polyethelene balloons to altitudes of the order of 20 millibars. The data was telemetered to ground or shipboard receiving stations and recorded on a mechanical oscillograph. Two counters were used on each flight and their pulses were fed through carefully matched sets of circuitry. These circuits were originally developed at New York University. Detailed descriptions of the counters and circuits have already been published.[2,15] To obtain better statistics, however, than those obtained from the earlier flights of this laboratory,[3–5] a separate circuit train was used for each counter instead of a single train and programming motor to switch from one counter to the other. The block diagram of the present arrangement is shown in Fig. 1.

NEUTRON DETECTION

In the past, it has been assumed[10] that most of the free neutrons in the atmosphere are slowed down to an energy where the only reaction that has an appreciable cross section for neutron capture is the one for the production of radiocarbon, namely,

$$ {}_0n^1+{}_7N^{14}\rightarrow {}_6C^{14}+{}_1H^1. \qquad (1)$$

However, it has been recently shown[16] that a not inconsiderable number of neutrons may be captured before they are slowed down to the energy range where the cross section for the above reaction becomes appreciable. Some of these fast neutrons are captured to form tritium by the reaction

$$ {}_0n^1+{}_7N^{14}\rightarrow {}_6C^{12}+{}_1H^3. \qquad (2)$$

There is also a small amount of resonance capture by nitrogen of neutrons in the Mev energy range that leads to radiocarbon production.[17] In this paper we shall neglect these higher energy reactions since the present data are limited by the fact that a boron detector has a very small capture cross section for neutrons in the Mev range.

We shall, therefore, adopt the procedure of former investigators,[3,4] and consider only the reaction of Eq. (1) for neutrons with energies less than 0.5 Mev. This upper limit is chosen because it is below the first resonance peak in the nitrogen cross-section curve.[18] We must bear in mind, however, that the results which are obtained using this assumption do not include fast-neutron capture.

The capture rate of neutrons at any point in the atmosphere can be calculated from the counting rate of a counter at that point by the equation[10]

$$ q=780n/V_c p_{0c}(\sigma_a(v)/\sigma_c(v)) \text{ captures g}^{-1}\text{ sec}^{-1}, \qquad (3)$$

where n is the counting rate of the counter; V_c is the active volume of the counter; p_{0c} is the pressure in atmospheres of the filling gas at 0°C; and $\sigma_a(v)$ and $\sigma_c(v)$ are the capture cross sections for air and the counter filling gas, respectively. Equation (3) is a simple multiplication procedure when σ_a and σ_c both vary as $1/v$. With the aid of this equation we can now compute the number of neutrons of energies less than 0.5 Mev (the $1/v$ energy region for N^{14} and B^{10}) absorbed per gram per second in the earth's atmosphere by the reaction of Eq. (1) if we know the observed counting rate of a BF_3 counter.

In the region of the atmosphere between 200 and 700 mb, which is the exponential portion of the neutron intensity *versus* atmospheric pressure curve, equilibrium exists. Further, it has been shown[4] that the average distance a neutron will diffuse during the time it spends slowing down to thermal velocity in the atmosphere is of the order of one kilometer. Therefore, all of the neutrons produced in this region will be captured within about a kilometer of the point of production. It follows that in this equilibrium region, q will be the production rate of those neutrons which are detected. To get the total neutron production, one would have to add to this q value all of the neutrons which are captured before they are slowed down to energies below 0.5 Mev.

Thus far, we have tacitly assumed that we have an ideal $1/v$ detector which counted only those neutrons which it captured. We shall now show how this ideal detector was approximated in practice. We know that in the energy range being considered, the boron (the

[15] Pavalow, Davis, and Staker, Rev. Sci. Instr. 21, 529 (1950).
[16] E. L. Fireman, Phys. Rev. 91, 922 (1953).
[17] R. K. Adair, Revs. Modern Phys. 22, 249 (1950).
[18] *Neutron Cross Sections*, Atomic Energy Commission Report AECU-2040 (Technical Information Service, Department of Commerce, Washington, D. C., 1950) and supplements.

B^{10} isotope) capture cross section varies little from a $1/v$ relation. However, high-energy neutrons will produce recoils that will cause counts, and other large cosmic ray events will be recorded from time to time. This background can be subtracted in various ways. The technique used in these experiments was first developed by Staker[3] and Davis.[4]

As was mentioned in the preceding section, two counters were used for each flight. These were identical in construction and filled to the same pressure with BF_3 gas. They differed only in the isotopic ratio of $B^{10}F_3$ to $B^{11}F_3$. One was filled with enriched BF_3 (96% B^{10}),[19] while the other was filled with normal BF_3 (19% B^{10}).[20]

If two such counters are exposed to the same particle flux, consisting of fast and slow neutrons, and other cosmic ray events, then the total number of counts recorded by the enriched counter would be

$$A = 0.96N + b \quad \text{counts min}^{-1}, \tag{4}$$

while the unenriched counter would record

$$B = 0.19N + b \quad \text{counts min}^{-1}, \tag{5}$$

where N is the theoretical neutron counting rate for

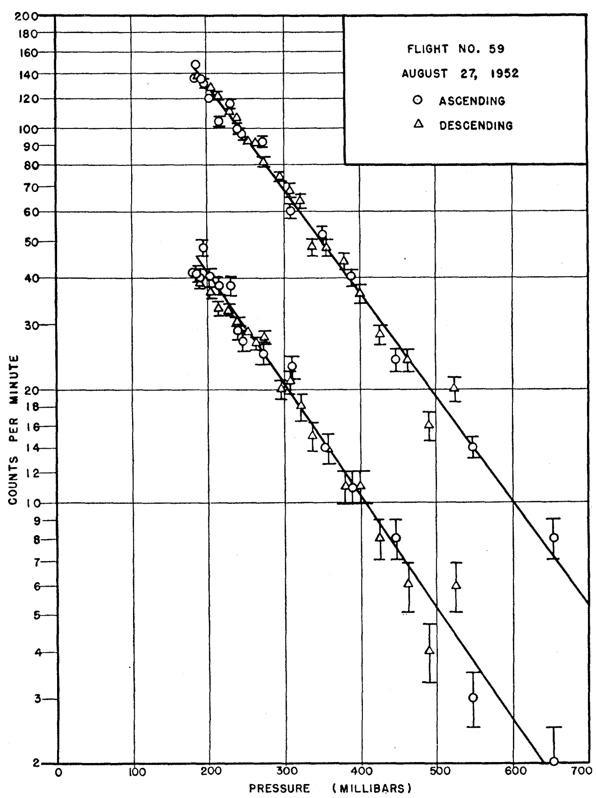

FIG. 2. Individual counting rates *versus* pressure. Flight No. 59. The upper curve represents the data for the enriched BF_3 counter, and the lower curve the data for the unenriched BF_3 counter.

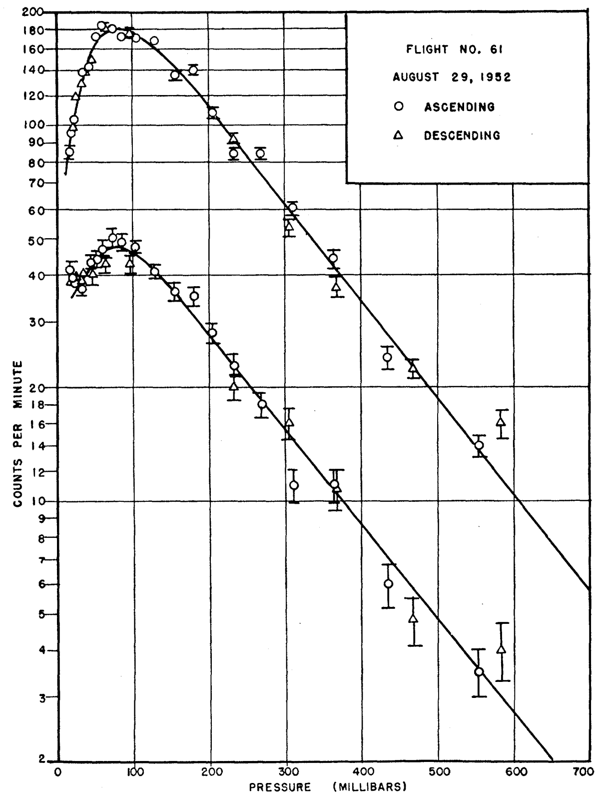

FIG. 3. Individual counting rates *versus* pressure. Flight No. 61. The upper curve represents the data for the enriched BF_3 counter, and the lower curve the data for the unenriched BF_3 counter.

such a counter that contains 100% $B^{10}F_3$, and b is the background counting rate. Solving these two equations, we obtain the following for N and b:

$$N = 1.3(A - B) \quad \text{counts min}^{-1}, \tag{6}$$

$$b = B - 0.19N \quad \text{counts min}^{-1}. \tag{7}$$

Since the $B^{11}F_3$ is assumed to be equally as effective as the $B^{10}F_3$ for counting background events, the b in Eqs. (4) and (5) is the same, and is directly determined in the observations.

EXPERIMENTAL RESULTS

For the present experiments, ten balloon flights were made at three different geomagnetic latitudes. These latitudes were 88.6°N, 10.1°N, and 55.1°N. Of these ten flights, seven were either completely or partially successful in that they yielded useful data. The first two successful flights at 88.6°N have already been fully described.[2]

The second series of flights was launched during the summer of 1953 from the *U. S. S. Currituck*, a United States Navy sea plane tender. The balloons were launched from the vicinity of the Galapagos Islands in the Pacific Ocean off the coast of Ecuador.

The first flight of this series (Flight 63) was launched at 8:09 A.M., C. S. T. on September 6, 1953 using a 90-

[19] Obtained from the U. S. Atomic Energy Commission, Oak Ridge, Tennessee.

[20] R. Stephenson, *Introduction to Nuclear Engineering* (McGraw-Hill Book Company, Inc., New York, 1954).

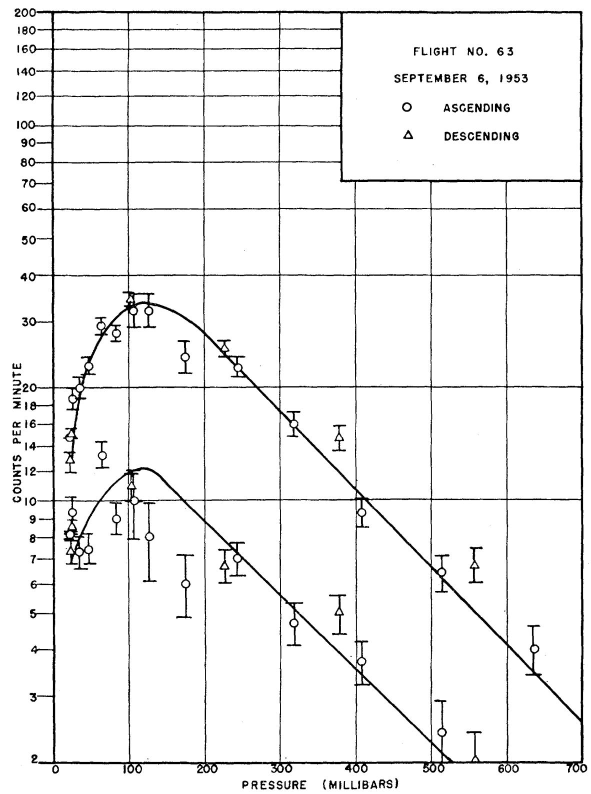

FIG. 4. Individual counting rates *versus* pressure. Flight No. 63. The upper curve represents the data for the enriched BF_3 counter, and the lower curve the data for the unenriched BF_3 counter

foot polyethelene balloon. The ship's position in geographic coordinates at the time of launching was 00° 16′S and 90° 21′W. The balloon rose at approximately 950 ft/min to an altitude of about 83 000 ft and then leveled off and floated at 85 000 ft for 2.3 hours. At this time a clock operated squib caused the gondola to be released on a parachute which descended in 0.5 hour. The total flight time was about 4.5 hours and data was recorded throughout this period.

Flight 64, the second of this series was launched at 10:08 A.M., C. S. T. on September 8, 1953. This flight, which used an 85-foot polyethelene balloon, was launched from geographic position 00° 16′S and 90° 19′W. The balloon rose at approximately 600 ft/min to an altitude of 20 000 ft. At this altitude the rate of rise increased to about 1000 ft/min until an altitude of 84 200 ft was reached, where the balloon leveled off and floated for the next two hours. At the end of this time, the signal-to-noise ratio decreased to the point where the transmitter signal became completely unintelligible. It is believed that the clock-operated squib must have cut the flight frame loose on a parachute at that time (since the flight frame was seen to come down during the next 0.5 hour), and in the shock of being dropped, the transmitting antenna was shorted to the frame. However, useful data were recorded for the 3.8 hours during which the balloon rose and floated at altitude.

The last flight of this series, number 65, was launched at 8:25 A.M., C. S. T. on September 9, 1953. The ship's position at the time of launching was 00° 19′S and 90° 22′W geographic coordinates. An 85-foot polyethelene balloon was used for this flight. The balloon rose at the rate of 750 ft/min to an altitude of about 33 000 ft, where the rate of ascent increased to 900 ft/min until it reached 77 000 ft. At this altitude it began leveling off and floated at about 80 000 ft for the next 2.5 hours. At 12:27 P.M., C. S. T., the clock-operated squib fired and released the flight frame on a parachute. The frame descended to the ground in the next 40 minutes. This flight lasted a total of 4.8 hours and data was recorded throughout this time.

The final series of flights in these experiments was made during the summer of 1954 from Fleming Field in South St. Paul, Minnesota. Since these flights were launched from land the launching position was fixed at 44° 54′N and 93° 08′W geographic coordinates. Flight 66, the first from Fleming Field, was launched at 6:49 A.M., C. S. T. on August 24, 1954. A 75-foot plastic balloon was used to carry the flight frame. This balloon rose at an average rate of 700 ft/min to an altitude of 85 000 ft. However, when the balloon reached 39 000 ft,

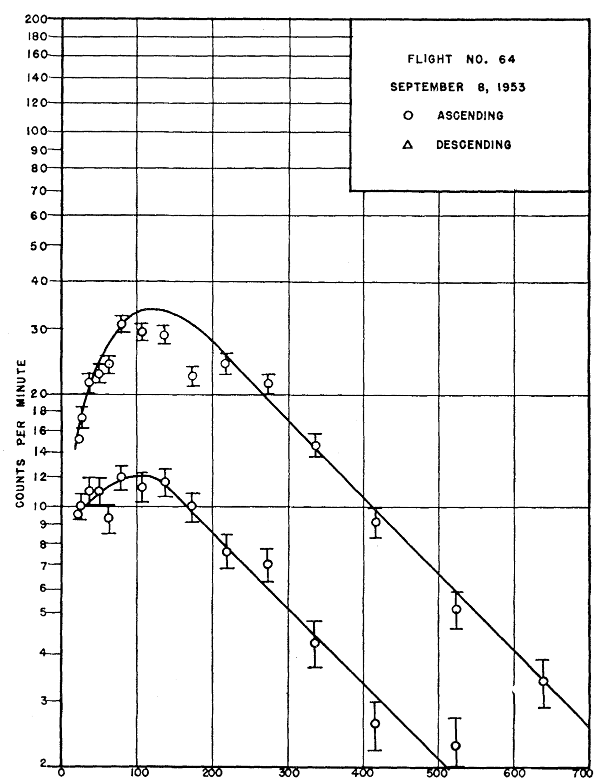

FIG. 5. Individual counting rates *versus* pressure. Flight No. 64. The upper curve represents the data for the enriched BF_3 counter, and the lower curve the data for the unenriched BF_3 counter.

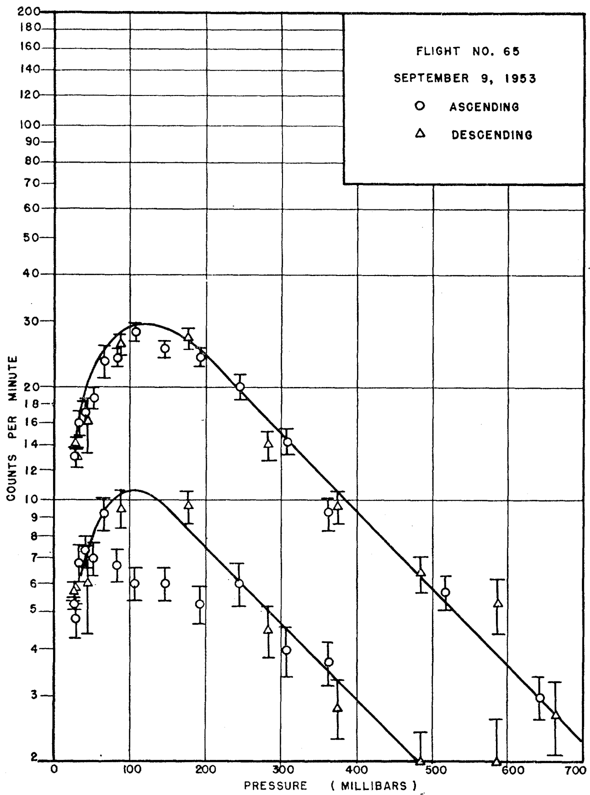

FIG. 6. Individual counting rates *versus* pressure. Flight No. 65. The upper curve represents the data for the enriched BF_3 counter, and the lower curve the data for the unenriched BF_3 counter.

pulses from the enriched counter ceased. Therefore, the remaining data received past that point was discarded. Useful data was obtained, therefore, for only 0.8 hour.

Flight 67 was launched at 6:55 A.M., C. S. T. on August 28, 1954, also from Fleming Field. Another 75-foot balloon was used for this flight. It rose at about 1100 ft/min to an altitude of 88 000 ft and floated there for about 2 hours. At this time, a clock-operated squib blew a hole of predetermined size in the top of the balloon and it started to descend slowly. At an altitude of 75 000 ft the pulses from the regular counter started coming in erratically and shortly afterwards ceased coming in entirely. When the frame was recovered it was found that a lead in one of the amplifiers had come loose. However, reliable data were recorded for 4.6 hours.

On the basis of the launch sites and the drift of the balloons, a mean geographic position for each of the three series of flights was determined. These are 77.8°N and 73.5°W for the flights off the Greenland coast; 00.5°S and 91.8°W for the flights off the coast of Ecuador, and 44.9°N and 93.1°W for the flights from South St. Paul, Minnesota. These correspond to geomagnetic latitudes of 88.6°N, 10.1°N, and 55.1°N.[21]

[21] D. J. X. Montgomery, *Cosmic Ray Physics* (Princeton University Press, Princeton, 1949).

The data from all the wholly or partially successful flights, namely, flights 59, 61, 63, 64, 65, 66, and 67, have been plotted in Figs. 2 through 14. Figures 2 through 7 are the curves of the counting rates of the individual counters *versus* pressure (since the pressure is more significant in diffusion theory than the physical altitude) for each of the flights, with the one exception that the data from flights 66 and 67 have been plotted together on one set of curves (Fig. 7) since not enough data were obtained from flight 66 to make a separate set of curves worthwhile.

In Figs. 8 through 13 the neutron counting rates, as calculated by Eq. (6), are shown for each flight (with flights 66 and 67 plotted together). Finally the neutron counting rates for all the flights are shown in Fig. 14 for comparison. From Fig. 14, the neutron counting rates at the maximum, the position of the maximum ($\theta_{\max}$), and the slope of the equilibrium portion μ (the mean absorption coefficient if we assume the relation $N=N_0e^{-\mu p}$ for this portion of the curve), can be quickly obtained. These are tabulated in Table I.

The curves for flights 59 and 61 (Figs. 2, 3, 8, and 9) have been previously published.[2] However, the probable errors which were presented in that earlier publication have since been recalculated and are shown here in their corrected form.

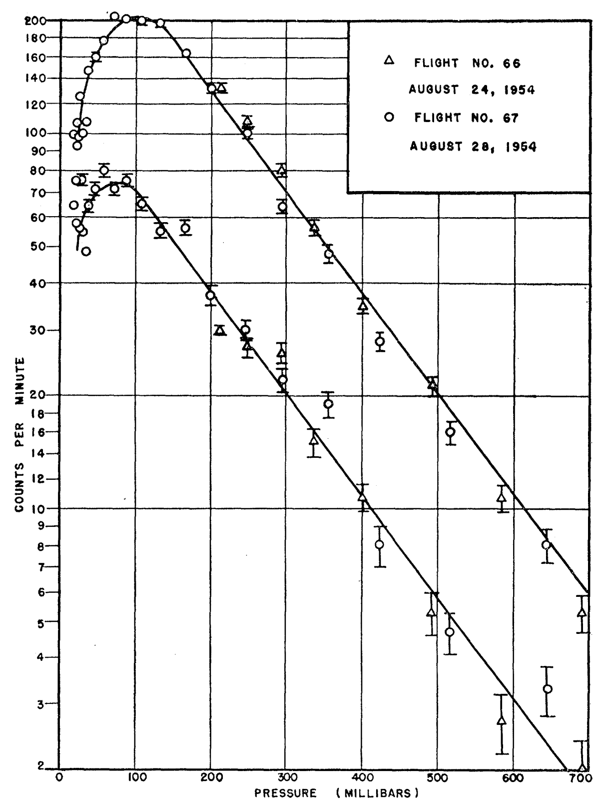

FIG. 7. Individual counting rates *versus* pressure. Flights No. 66 and 67. The upper curve represents the data for the enriched BF_3 counters, and the lower curve the data for the unenriched BF_3 counters.

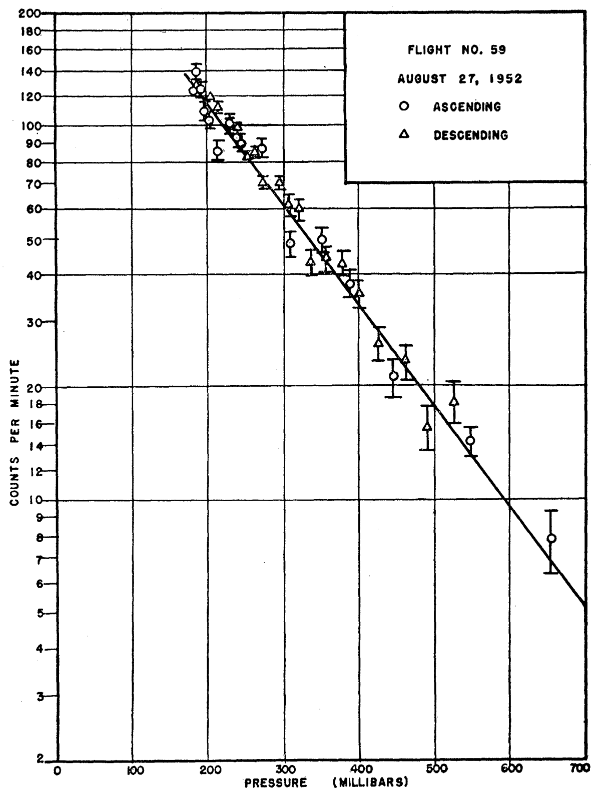

FIG. 8. Neutron counting rates *versus* pressure. Flight No. 59.

In a number of the experimental and derived curves shown above, particularly those for $\lambda = 10.1°$, it is noticed that in the range of 100 mb $< p <$ 200 mb, a number of points lie below the smooth curve which has been drawn. The reason for not considering these points in plotting the curves and a possible explanation to account for these points has been discussed in a previous paper.[14]

From the data of various sea level and mountain altitude stations that continuously monitor the cosmic-ray neutron flux in this hemisphere,[22] it was determined that all of the flights which were reported in this paper were flown on days when no variations greater than 1 percent were observed in the cosmic-ray neutron flux.

DISCUSSION

The foregoing results, as plotted in Fig. 14, can now be combined with the results of other investigators to yield a complete picture of the variations of cosmic-ray neutron intensity with atmospheric pressure and geomagnetic latitude. We shall concern ourselves here with atmospheric pressures of less than 700 mb, and neutrons of energy less than 0.5 Mev.

In the following sections we shall consider the variations of the salient features of the curve of neutron intensity *versus* pressure with geomagnetic latitude. As was stated in the introduction, these are (a) the variation of intensity at a constant pressure in the equilibrium portion of the atmosphere; (b) the variation of the mean absorption length L (or its inverse, the mean absorption coefficient μ); and (c) the change in position of the neutron intensity maximum. Having obtained the above variations, we shall then attempt to construct a family of curves which would show the neutron intensity variations with atmospheric depth at any geomagnetic latitude in the northern hemisphere (since the majority of available data was obtained in this hemisphere), and from these curves, try to obtain a lower limit for the world neutron production rate.

A. Geomagnetic Variation of the Neutron Intensity at Constant Atmospheric Depth or Pressure

Simpson[11] and Yuan[12] have measured the latitude dependence of fast and slow neutrons at a constant atmospheric depth, using BF_3 counters with various shielding arrangements flown in B29 aircraft. Their results are in agreement as to the general form of the variation and the relative intensities. There is also agreement within experimental error between the relative intensities which they obtained and the points taken from the experiments reported here. This is to be expected since the energy spectrum of atmospheric neutrons below the intensity maximum does not appear

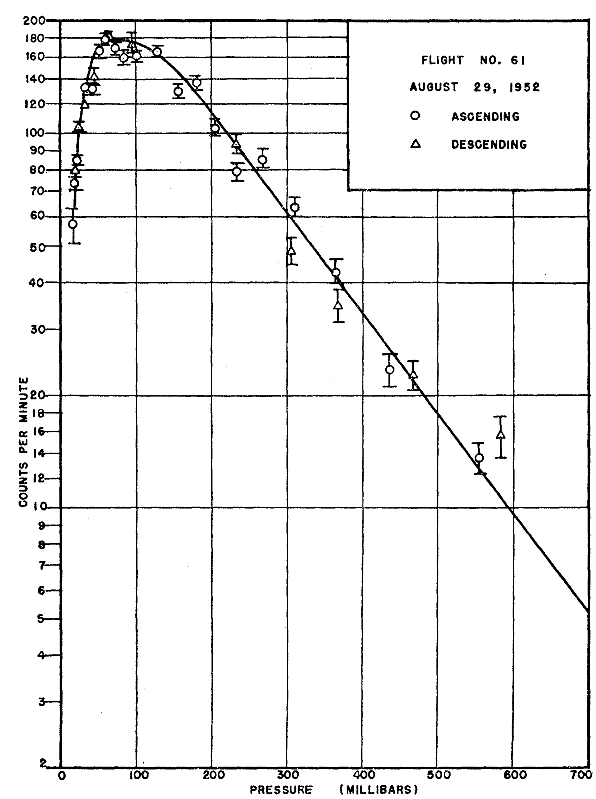

FIG. 9. Neutron counting rates *versus* pressure. Flight No. 61.

[22] J. A. Simpson (private communications).

TABLE I. Results of the present series of experiments.

Geomagnetic latitude (λ)	Maximum counting rate (cpm)	Position of the maximum (θ_{max}) (mb)	Mean absorption coefficient (μ) (mb^{-1})	Mean absorption length[a] (L) (g/cm^2)[b]
88.6°	180	75±5	0.0062	164
55.1°	180	100±5	0.0062	164
10.1°	30	120±5	0.0048	212

[a] The mean absorption length, L, is related to the mean absorption coefficient, μ, by $L=1/\mu$.
[b] These are the units in which the mean absorption length is commonly expressed.

to change with altitude[23] or latitude.[24] This is also in agreement with the theory since this energy distribution arises from the scattering, slowing-down, and capture of neutrons by nitrogen and oxygen and does not depend strongly on the initial kinetic energy of the neutrons. A complete discussion of this slowing-down and capture process has been given by Bethe, Korff, and Placzek.[10] Therefore, in the equilibrium portion of the atmosphere, between pressures of 200 and 700 mb the distribution of fast-neutron intensities is the same as the distribution of slow-neutron intensities. Thus, in this region of the atmosphere we can justify the use of relative intensity data obtained with different shielding arrangements around the BF_3 counters if we normalize to the present counter arrangement.

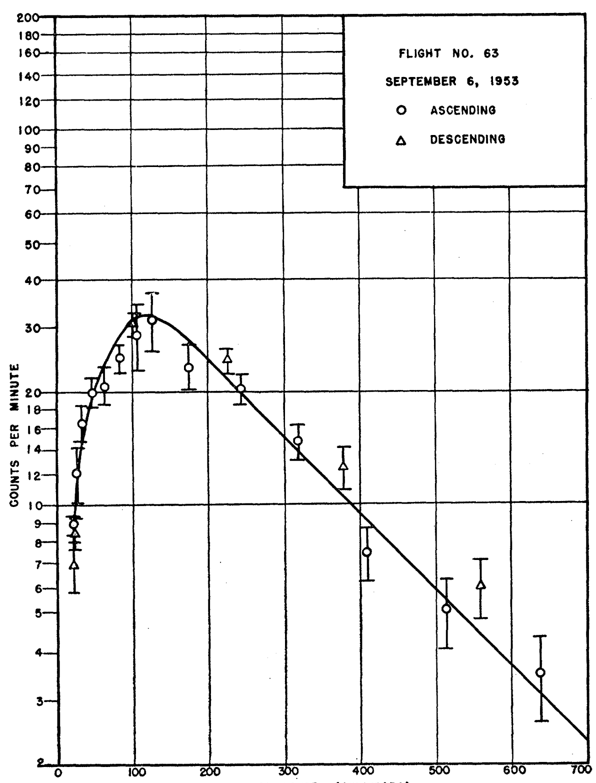

FIG. 10. Neutron counting rates *versus* pressure. Flight No. 63.

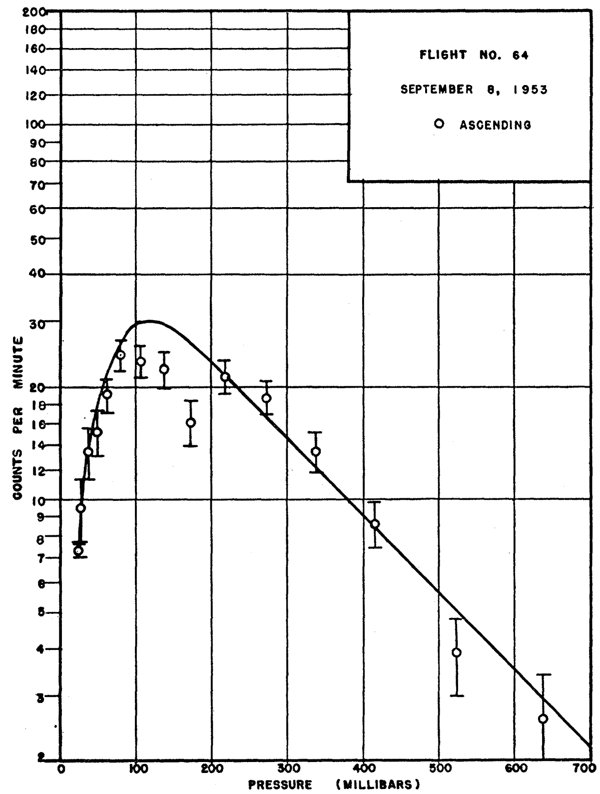

FIG. 11. Neutron counting rates *versus* pressure. Flight No. 64.

For the purposes of this paper it was decided to use the curve reported by Simpson,[11,25] since it covers a greater latitude range than the curve obtained by Yuan[12] and also because it was determined that the curve to be used was drawn from data obtained on days when there were no large fluctuations from the norm in the neutron intensity. This curve is reproduced in Fig. 15.

B. Variation of the Mean Absorption Length with Geomagnetic Latitude

As was mentioned previously, the neutron intensity distribution in the equilibrium region of the atmosphere can be approximated by the following relation:

$$N=N_0e^{-p/L}=N_0e^{-\mu p}, \tag{8}$$

where L is called the mean absorption length and μ the mean absorption coefficient. Table II lists the more recently reported values of L and μ at various geomagnetic latitudes as well as the values derived from the present experiments. The values which were obtained by Staker[3] and Staker, Pavalow, and Korff[5] have been re-evaluated on the basis of a more detailed study

[23] Agnew, Bright, and Froman, Phys. Rev. **72**, 203 (1947).
[24] Simpson, Baldwin, and Uretz, Phys. Rev. **76**, 165 (1949).
[25] Simpson, Fonger, and Treiman, Phys. Rev. **90**, 934 (1953).

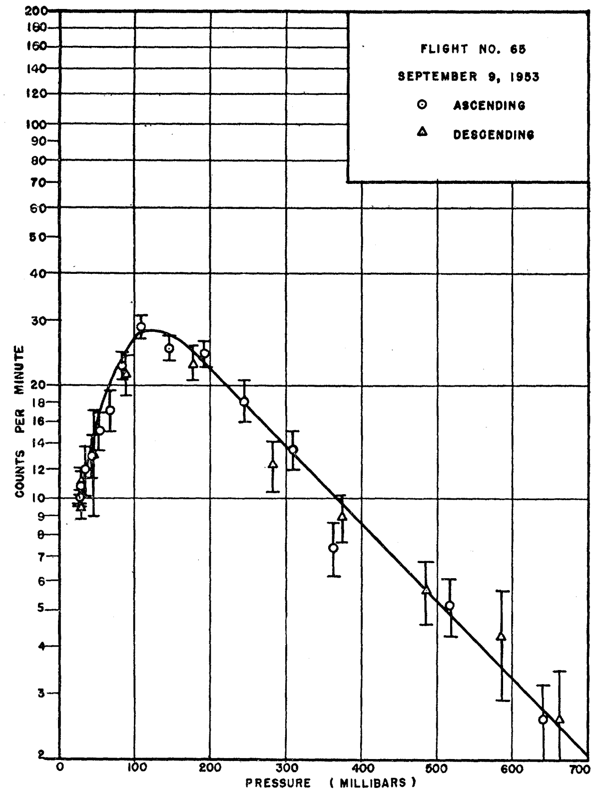

FIG. 12. Neutron counting rates *versus* pressure. Flight No. 65.

of the original data and these corrected values are listed in Table II.

Figure 16 shows the curve obtained by plotting these values of μ as a function of geomagnetic latitude. It should be noticed that where several investigators have reported values at nearby latitudes, these agree to within experimental error despite the fact that Yuan[13] was measuring only slow-neutron intensities ($E<0.4$ ev), Simpson[11] was measuring only fast neutron intensities, and the values reported here as well as those of Staker[3] and Staker *et al.*,[5] were obtained from measurements on a combination of fast- and slow-neutron intensities. This again points up the fact that in the equilibrium region of the atmosphere the variations of neutron intensity are independent of the energy range being considered.

TABLE II. Mean absorption length and mean absorption coefficient *versus* geomagnetic latitude.

Geomagnetic latitude (λ)	Mean absorption length (L) (g/cm²)	Mean absorption coefficient (μ) (mb⁻¹)	Reference symbol
0°	212	0.0048	a
10.1°	212	0.0048	b
19°	206	0.0050	a
30.4°	196	0.0052	c (corrected)
40°	181	0.0056	a
51°	156	0.0065	d
53°	157	0.0065	a
54.7°	162	0.0063	c (corrected)
55.1°	164	0.0062	b
65°	157	0.0065	a
69°	162	0.0063	e (corrected)
88.6°	164	0.0062	b

[a] J. A. Simpson, Phys. Rev. **83**, 1175 (1951).
[b] Present experiments.
[c] W. P. Staker, Phys. Rev. **80**, 52 (1950).
[d] L. C. L. Yuan, Phys. Rev. **81**, 175 (1951).
[e] Staker, Pavalow, and Korff, Phys. Rev. **81**, 889 (1951).

It is clear from the curve in Fig. 16 that the latitude dependence in the neutron intensity demonstrates that the neutrons are produced either directly or indirectly by incident primary charged particles. For, as the average energy of the incident primaries increases, the number and average energy of the nucleonic secondaries will also increase. Thus the nucleonic cascades will extend to greater depths and the star production per nucleon will increase. Therefore, the mean absorption length of the neutrons which are produced in these stars should vary directly as the average incident primary energy. Because of the geomagnetic cutoff, one would expect the total incident primary intensity to vary inversely as the average energy of these primaries. Thus, the mean absorption coefficient, which is the inverse of the mean absorption length, should vary directly as the total incident primary intensity. The foregoing seems to be borne out by the similarity between the curve of Fig. 16 and the reported curve for

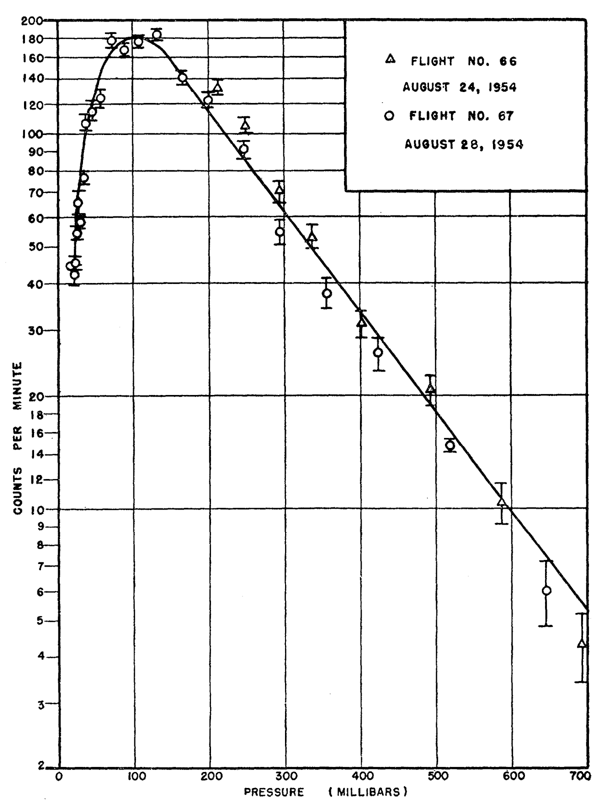

FIG. 13. Neutron counting rates *versus* pressure. Flights No. 66 and 67.

the incident primary intensity.[26] Both curves have the same general shape with a "knee" at about the same geomagnetic latitude although the "knee" in the curve of Fig. 16 appears to be more abrupt than that reported for the incident primaries.

C. Position of the Neutron Intensity Maximum as a Function of Geomagnetic Latitude

This topic has already been treated in detail in a previous publication.[14] For the purposes of this paper it is necessary only to present the graphical results which were derived in that earlier work. This is done in Fig. 17 which shows the variation of the position of the neutron intensity maximum ($\theta_{\max}$) with geomagnetic latitude.

D. Neutron Intensities at High Altitudes in the Northern Hemisphere

Having investigated the latitude variation of the salient features of the curves of neutron intensity *versus* pressure, we are now in a position to construct a family of such curves for all geomagnetic latitudes in the northern hemisphere. These curves will be normalized to conform to the experimental data presented earlier.

With the aid of the curve of neutron intensity at

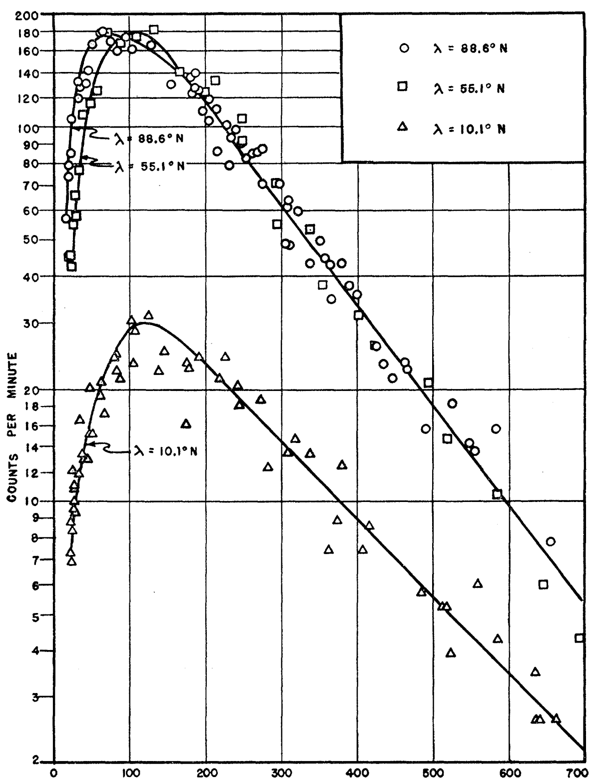

FIG. 14. Composite curves of neutron counting rates *versus* pressure for the three latitudes studied.

[26] Biehl, Neher, and Roesch, Phys. Rev. **76**, 914 (1949).

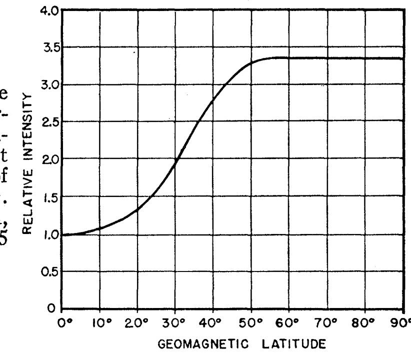

FIG. 15. Relative neutron intensity *versus* geomagnetic latitude for a constant atmospheric depth of 312 g/cm² (306 mb). From J. A. Simpson, Phys. Rev. **83**, 1175 (1951).

constant atmospheric pressure (Fig. 15) and the latitude variation of the mean absorption coefficient (Fig. 16), we can construct the curves for the equilibrium region of the atmosphere (200 to 700 mb) after normalizing to the experimental curve obtained at $\lambda = 10.1°$ (Fig. 14). For the top of the atmosphere (above 200 mb) the shape of the curve at any geomagnetic latitude can be extrapolated from the experimental curves of the previous section and also from those of Staker,[3] Davis,[4] and Staker *et al.*[5] The position of the maximum is read from the curve in Fig. 17. It should be noticed that the form of these curves at pressures less than about 20 mb is merely extrapolated and should be viewed in that light.

Figure 18 shows just such a family of curves plotted for intervals of ten degrees geomagnetic latitude from the geomagnetic equator to the pole. To avoid confusion, the curves for 70° and 80° are not shown in this figure. However, from the foregoing discussion it can be seen that these curves would be identical to those for 60° and 90° below 200 mb, and that they would fall between the 60° and 90° curves above 200 mb.

From these curves we can now calculate the low-energy neutron absorption rate at any altitude and latitude. As discussed in the section on neutron detection, this would be a lower limit to the cosmic ray neutron production rate. We showed in that section that

$$p = n\sigma_a\, 780/V_c\sigma_c p_{0c}\ \text{g}^{-1}\ \text{sec}^{-1}, \qquad (3)$$

where, for the present apparatus: $V_c = 575$ cm³, $p_{0c} = 23.2$ cm Hg $= 0.307$ atmos, and $n = N/60$ sec^{-1}, since N is expressed in units of min^{-1}.

For 100 percent $B^{10}F_3$, the boron capture cross section, σ_c can be expressed as 631 $E^{-\frac{1}{2}}$ barn.[20] The capture cross section of nitrogen for neutrons of energy less than 0.5 Mev can be expressed as 0.269 $E^{-\frac{1}{2}}$ barn.[18,20] From this, we can express the capture cross section of air as $\sigma_a = 0.430\ E^{-\frac{1}{2}}$, and by substituting these values in Eq. (3), we obtain the relation

$$q = 5.01 \times 10^{-5} N\ \text{g}^{-1}\ \text{sec}^{-1}, \qquad (9)$$

with which we can now convert the counting rates to absolute values.

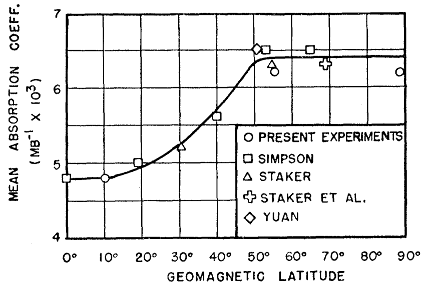

FIG. 16. Mean absorption coefficient *versus* geomagnetic latitude.

E. Total Cosmic-Ray Neutron Intensities

It is of interest to determine the integrals under the curves of Fig. 18, since from these and Eq. (9) we can obtain the total number of neutrons of energy less than 0.5 Mev absorbed per second per square centimeter of the earth's atmosphere by the $N^{14}(n,p)$ reaction. This should be at least a lower limit to the total number of neutrons produced per second per square centimeter of the earth's atmosphere.

The curves of Fig. 18 were graphically integrated with the region below 700 mb extrapolated. While Simpson and Fagot[27] have shown that such an extrapolation is not strictly valid, its use here introduces very little error in the total integration. These results were then expressed, with the aid of Eq. (9), as the integrated neutron absorption in a square centimeter column per second (i.e., $\int qdp = Q_\lambda$) and plotted as a function of geomagnetic latitude (see Fig. 19). It is noted that this curve has the same shape as the integrated charged particle intensity curve which has been reported by other investigators.[28] There is a cutoff in the incoming primary spectrum at about 1.5 Bev, if one assumes the geomagnetic cutoff values for vertically incident protons.[29] This is in good agreement with recent direct measurements on the primary spectrum.[30] Above this "knee" it can be seen that the curve continues to rise at a much lower rate. This rise is entirely due to the shift of the height of the neutron maximum at latitudes greater than about 55°. This shift and consequent rise in intensity is probably due to a small number of low-energy primaries which are incident at those latitudes and create nucleonic cascades which do not extend to pressures greater than about 100 mb. This seems to be an indication that the cutoff in the primary energy spectrum at about 1.5 Bev is not complete and that a small number of primaries with energies less than about 1.5 Bev do reach the earth's upper atmosphere. It can also be seen from Fig. 19 that the latitude variation in the cosmic-ray neutrons is about 420% which is much larger than the 250% variation reported for the integrated total intensity of the charged particles.[28]

[27] J. A. Simpson and W. C. Fagot, Phys. Rev. **90**, 1068 (1953).
[28] Neher, Peterson, and Stern, Phys. Rev. **90**, 655 (1953).
[29] R. A. Alpher, J. Geophys. Res. **55**, 437 (1950).
[30] J. A. Van Allen, Nuovo cimento **10**, 630 (1953).

It is of interest to compare the values of q and Q_λ obtained here with those obtained by other investigators. Simpson[11] reports a value for q of $(3.2\pm0.05)\times10^{-3}$ g^{-1} sec^{-1} at an atmospheric depth of 312 g/cm^2 and $\lambda=0°$ while at the same atmospheric depth and latitude, a value of 0.7×10^{-3} g^{-1} sec^{-1} is obtained by applying Eq. (9) to the curves of Fig. 18. The most recent calculation[31] on the data from the balloon flights of Yuan[13] yield a value of $Q_\lambda=3.50$ cm^{-2} sec^{-1} at $\lambda=52°$. From Fig. 19, we see that the present work gives a value of 1.9 cm^{-2} sec^{-1} at the same latitude. The discrepancy between these values is due to the different methods of calculating q from the observed counting rate. Both Simpson and Yuan calculated q from observations upon restricted portions of the neutron energy spectrum. They then extrapolated the total neutron intensity from these observations. To do this, an energy distribution for the cosmic-ray neutrons in the atmosphere had to be assumed. While the present observations are heavily weighted with slow neutrons, no energy distribution assumptions were necessary for the calculations. A more recent measurement by Ortel[32] on the production rate of neutrons at $\lambda=39°$ and an atmospheric depth of 675 g/cm^2 yielded a value of 3×10^{-4} g^{-1} sec^{-1}, which is in fair agreement with the value of 2.5×10^{-4} g^{-1} sec^{-1} which we obtained for q at that depth and latitude.

The large latitude effect we observe in Fig. 19 might at first glance also lead us to expect a large latitude effect for the radiocarbon found in nature, since the Q_λ values considered are for neutrons captured by the $N^{14}(n,p)$ reaction which results in the production of radiocarbon. However, as Anderson and Libby[33] have pointed out, C^{14} with a half-life of 5570 years has ample time to be thoroughly mixed by air and water currents before being fixed. They give this as the reason why no such large latitude effect in the C^{14} abundance is found.

It is now possible to integrate the values of Q_λ over the surface of the earth. It is assumed that the neutron

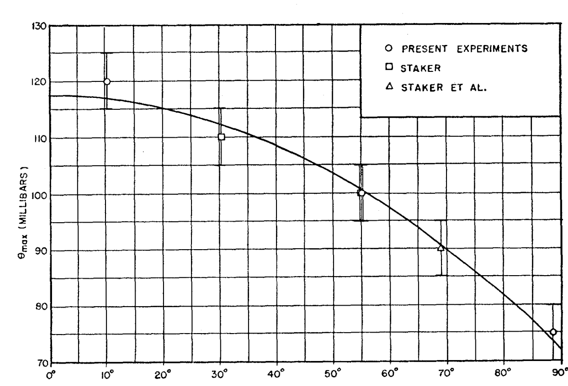

FIG. 17. Position of the neutron intensity maximum *versus* geomagnetic latitude.

[31] H. J. Kouts and L. C. L. Yuan, Phys. Rev. **86**, 128 (1952).
[32] W. C. G. Ortel, Phys. Rev. **93**, 561 (1954).
[33] E. C. Anderson and W. F. Libby, Phys. Rev. **81**, 64 (1954).

intensity distribution is symmetric with respect to the geomagnetic equator. While it is presumed that there is a longitude effect in the high-altitude neutron intensity, within the limits of accuracy of this integration it is possible to consider the earth as a sphere with the geomagnetic dipole at its geographic center, and thus, that the neutron intensity is independent of longitude. Such an integration yields a value for the number of neutrons below 0.5 Mev captured by atmospheric nitrogen of $Q_T = 5.8\times10^{18}$ sec^{-1} or a mean value of $\bar{Q}_\lambda = 1.1$ neutrons captured per square centimeter column per second. Dividing Q_T by the disintegration rate of radiocarbon (4.0×10^{-12} sec^{-1}) and converting to mass units, this yields a lower limit for the amount of radiocarbon in equilibrium on the earth. This value is 34 metric tons. The total amount of radiocarbon should be slightly larger than this value because of the resonance captures of the $N^{14}(n,p)$ reaction in the energy range of 0.5 to 14 Mev.[17]

The value of $\bar{Q}_\lambda = 1.1$ cm^{-2} sec^{-1} may be compared with the observed number of β disintegrations from radiocarbon since, in equilibrium, these should be equal. Anderson and Libby[33] report this value as 2.23 disintegrations cm^{-2} sec^{-1} over the surface of the earth. Some more recent measurements[34,35] indicate that this

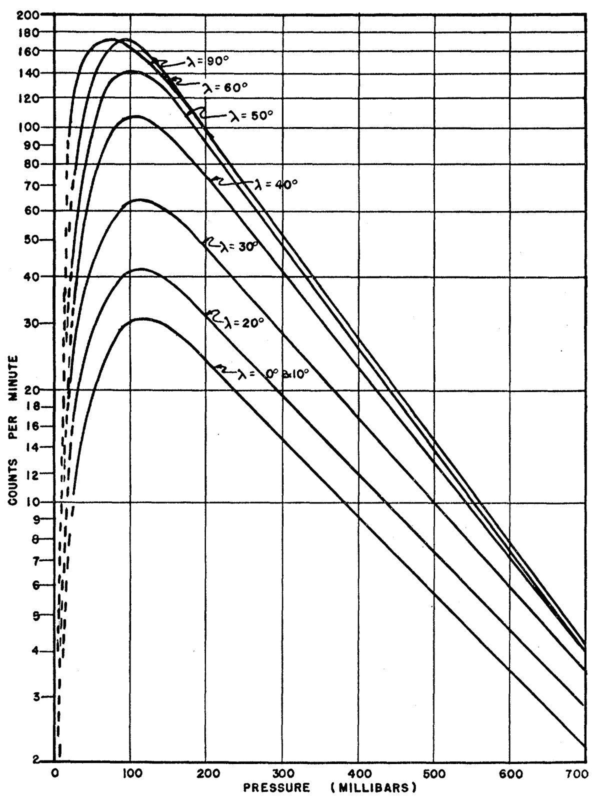

FIG. 18. Neutron intensity *versus* pressure for latitudes in the northern hemisphere.

[34] Hayes, Williams, and Rogers, Phys. Rev. **92**, 512 (1953).
[35] G. J. Ferguson, Nucleonics **13**, 18 (1955).

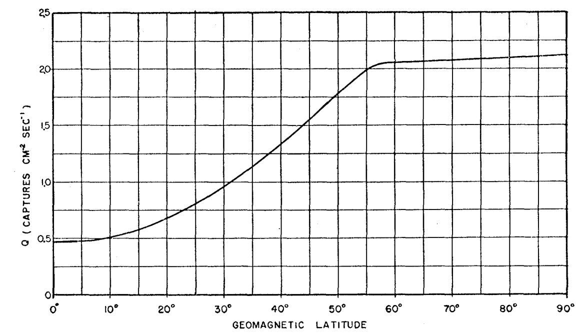

FIG. 19. Integrated neutron intensity *versus* geomagnetic latitude.

figure is too high. The present maximum figure from the radiocarbon work is 1.75 disintegrations cm^{-2} sec^{-1}. This figure will probably be revised downward by 5 to 15 percent when better data is available on the diluting action of the carbon supply in the oceans.[36] This is now in reasonable agreement with the value of 1.1 neutrons captured cm^{-2} sec^{-1} since this value is a minimum which does not take into account the radiocarbon formation by resonance captures of neutrons with energies greater than 0.5 Mev.

In conclusion it should again be pointed out that there is no conflict between the experimental data reported here and that of any of the experimenters whose measurements have been mentioned above. The numerical discrepancies pointed out in the preceding paragraphs arise in the calculation of the absolute neutron intensity from the results of the various experimental arrangements. The differences in the methods of calculation are large, and in some cases individuals have found values differing by factors of two or more from the same experiment.

ACKNOWLEDGMENTS

The author wishes to express his sincere gratitude to Professor S. A. Korff who proposed this problem, for his guidance and helpful suggestions. Thanks should also be given to Dr. Martin Swetnick and to Hugo Neuburg, Roy Elkind, Israel Schlechter, Arie Borovitch, Raymond Chang, and George Timmerman for their assistance in constructing the flight frames and in carrying out the flights; to Arthur Beiser for many stimulating discussions; and to Dr. J. A. Simpson of the University of Chicago for making his neutron monitoring data available.

In addition, the author wishes to express his indebtedness to the General Mills balloon group for the flights near the geomagnetic pole and at the Galapagos Islands; to the balloon group at Winzen Research, Inc. for the flights from St. Paul, Minnesota; to Captain O. A. Peterson and the officers and men of the *U. S. C. G. C. Eastwind* for their cooperation on the flights near the geomagnetic pole; and to Captain J. D. Black and the officers and men of the *U. S. S. Currituck* for their assistance on the flights from the Galapagos Islands.

[36] W. Broecker, private communication.